Direct Determination of Oxide Surface Free Energy through Potentiometric Measurements

Kevin Croué,[a,c] Jean-Pierre Jolivet,[b] and Dominique Larcher[a,c,z]

[a]*Laboratoire de Réactivité et Chimie des Solides, Université de Picardie Jules Verne, CNRS UMR6007, 80039 Amiens, France*
[b]*Université Pierre et Marie Curie-Paris 6 and CNRS, UMR 7574, Laboratoire de Chimie de la Matière Condensée de Paris, Collège de France, F-75005 Paris, France*
[c]*ALISTORE - European Research Institute, 80039 Amiens Cedex, France*

The total surface free energy of nanometric particles in contact with a liquid electrolyte can be easily accessed through potentiometric measurements. This requires a special though simple designed set-up, and a careful chemical and textural characterization of the powders. This is here first exemplified for non-stoichiometric NiO, in contact with Ni^{2+} aqueous solutions, which total surface free energy was evaluated to 0.34–0.36 J/m^2 for monolithic particles, independently of the level of non-stoichiometry. Much larger values are systematically observed for mosaic powders; hence indicating a large contribution of the solid-solid inter-crystallites interfacial energy or strains.
© 2011 The Electrochemical Society. [DOI: 10.1149/2.011201esl] All rights reserved.

Besides ab-initio methods,[1–3] many techniques are reported to measure surface energies but their entropic contribution is generally disregarded, and they are sometimes difficult to apply to highly divided materials.[4–7] Aside, EMF (Electro Motive Force) measurements are extremely compelling as they give direct access to the free excess energy and are very adaptable.[8,9] Strangely, despite the booming interest in nanometric materials, they have been seldom applied to the determination of their free surface energy[10] although attempts have been made to track crystal ripening.[11–15]

Our present strategy exemplifies this point and relies on the synthesis of non stoichiometric Ni oxides with controlled Ni/O stoichiometry (i.e. Ni^{+III} / Ni_{tot} ratio) oxide, particle size (i.e. specific surface area), and texture (i.e. mosaic vs. monolithic). Two electrodes, immersed in a liquid electrolyte containing Ni^{+2}, are comprising the same powder but in different amounts thus expressing known differences in surface area. Then, quasi-equilibrium EMF measurements between the electrodes are used to establish a relation with their surface/texture, and lead to the numerical determination of their surface and grain boundaries interface free energies.

The choice of this strategy is not fortuitous. In a Liquid-Liquid or Liquid-Gas interface, no bounding/crystallographic strain hinders bulk molecules from moving toward the surface to fulfil a newly created surface. For solids, the situation is relatively more complex as any increase in the surface of a distorting particle requires surface energy and surface strains to be separately considered. This has been the subject of long-lasting controversy[16] still making uneasy the interpretation of experimental data. Here, we do not consider any difference in size or particles radius; exactly the same powder is used at both electrodes. Initially, the system is perfectly symmetrical; the same amount of powder is placed at both electrodes. Then, we create an out-equilibrium state by withdrawing a part of the powder on one electrode. Going back to its equilibrium state implies that the system should evolve to reach a new symmetrical steady state. This potentially requires the dissolution of excess particles on one side, and precipitation of new ones containing Ni^{+III} on the other. As our electrolyte contains only Ni^{+2}, this process necessitates internal ion migration through the cell as well as external electron transfer (n), hence the measured EMF. The thermodynamic situation becomes:

$$\Delta G^{surf.} = \gamma_{total} \cdot \Delta A = nF\Delta E \quad \text{or} \quad \gamma_{total} = nF\frac{\Delta E}{\Delta A}$$

Experimental

The nickel oxalate gel was obtained by adding 50 mL of an ethanol solution of $Ni(NO_3)_2 \cdot 6H_2O$ (0.2 M) to 50 mL of an ethanol solution of $H_2C_2O_4 \cdot 2H_2O$ (1 M).[17] The resulting green gel was separated from the solution by repeated ethanol washings and centrifugation steps (6000 rpm, 10 min) and then dried at 80°C for 6 hours. Ni oxides were formed by heat-decomposition of the nickel oxalate ($NiC_2O_4 \cdot 2H_2O$) in air at 320°C with times ranging from 40 minutes to 34 hours. For sake of clarity, our annealed samples will therefore be labelled NiO $_{Time}$. A green stoichiometric $Ni^{+II}O$ bulk sample was prepared at 900°C for 12 hours.

Phase composition was determined by X-Ray Diffraction (XRD, Bruker D8 diffractometer, CuKα, λ = 1.54056 Å) equipped with a Position Sensitive Detector (PSD). Cell parameters were estimated by the ERACEL software[18] while the crystallite size (L_c) and structural strains (ε) were obtained from the Williamson-Hall formalism.[19] Specific surface areas were determined using the Brunauer–Emmett–Teller (BET) multipoint method[20] from N_2 physisorption at 77 K (Micromeritics). Particles sizes distributions were computed from statistical analysis of TEM images (TECHNAI) with at least 200 observations per sample. The nickel mean oxidation state (m.o.s) was determined by iodometric titration. The powder (50 mg) was dissolved in 6 M HCl aqueous solution containing KI excess (500 mg) and under N_2 flow. I_2 resulting from the oxidation of iodide by Ni^{3+} was back titrated with a $Na_2S_2O_3$ solution (10^{-2} M) using starch as end-reaction indicator. The total nickel contents were measured by titration with Na-EDTA and murexide as indicator (absolute incertitude = +/−0.04)

Electrochemical measurements were carried out at 20°C (maximum deviation = 0.01°C/h) (VMP, Biological, sciences instrument) in Open Circuit Voltage (OCV) mode. The Teflon-based Swagelok electrochemical cells were thermally and electromagnetically isolated by Dewar/polystyrene and copper grids wrappings. Blank measures show an OCV deviation less than 70 μV/30 minutes, thermostatic conditions being mandatory to avoid any thermocouple effects due to electric connexions with stainless steel plungers. Optimization of the OCV stability was found to require highly concentrated electrolyte and horizontally orientated cell to minimize the concentration gradient effects (Figure 1).

The oxide powders were hand-mixed with 5 wt% SP carbon for 10 min. Initially, 100 mg of this mixture was used at both electrodes, separated by glass fibre disks, the whole soaked with a 1 M aqueous solution of $NiSO_4 \cdot 6H_2O$.

After OCV stabilization (deviation < 50 μV/h), the cell was repeatedly opened and a small part of the powder mixture extracted from one side only. The extracted part was washed, dried and weighed to

[z] E-mail: Dominique.larcher@sc.u-picardie.fr
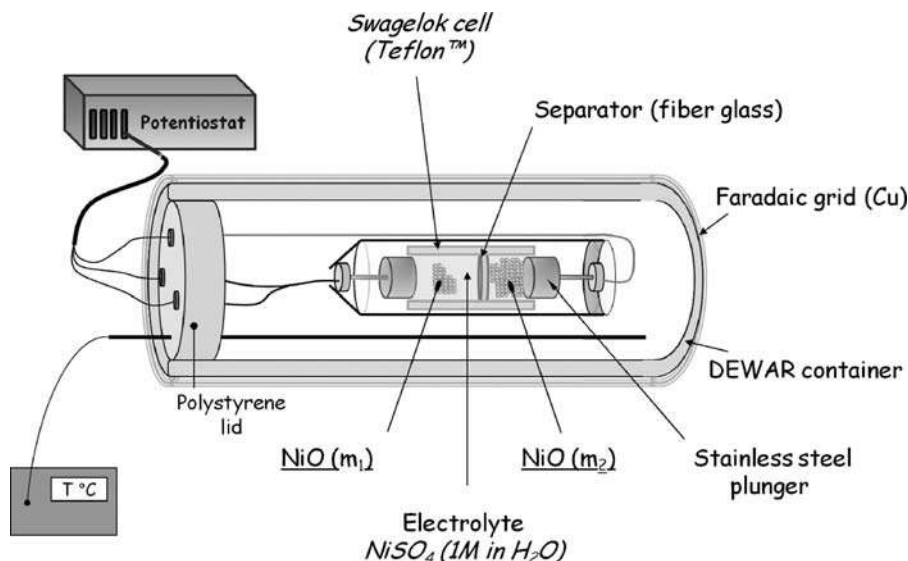
Figure 1. Details of our experimental potentiometric measure setup.

evaluate the withdrawn amount. For each cell, we verified (TEM, XRD) that the contact with the electrolyte did not affect either the structure, size, morphology or the stoichiometry of the powders within the duration of the experiment, *i.e.* no ripening/reaction.

Results and Discussion

After initial dehydration of the $NiC_2O_4 \cdot 2H_2O$ precursor into NiC_2O_4, the single NiO phase is formed beyond 40 minutes at 320°C (Figure 2). Their Ni m.o.s. was determined through both chemical titration and from cell parameter values, as the latter linearly evolves with stoichiometry.[21] According to these two matching methods, the Ni^{+III} content was found to range from 7% to 0.5%, decreasing as the heating time increases. All these samples are grey-black in contrast to greenish for stoichiometric NiO.

Analysis of the TEM images revealed nanometric spheroid particles (4.1–7.2 nm) with narrow size distributions (Figure 3). Oxide particles are necklace-like organized, retaining the filament shape of the precursor particles. BET values conversely decrease as the particles size drops and match their calculated geometrical specific surface demonstrating a very low porosity. However, in the case of a few sam-

ple, we spotted a mismatch between particle (L_p, TEM) and crystallite (L_c, XRD) sizes enlightening a monolithic texture for NiO $_{40\,min}$ and NiO $_{34\,h}$ samples ($L_c \sim L_p$) and a mosaic one for intermediate samples ($L_c < L_p$) (Figure 3). This is consistent with a coarsening of the particles with the presence of internal solid-solid interfaces for particles ongoing crystallites merging.

EMF (ΔE) was found to increase linearly with the difference in electrode surface area (ΔA) for each tested NiO sample (Figure 4), validating the first step of our methodology. Cells comprising only SP carbon and with various Ni/SP ratios do not reveal any apparent deviation, ruling out any effect of the conducting additive on the OCV values. Back to the basic of our approach, the $\Delta E = f(\Delta A)$ slope is proportional to the γ/n ratio, n standing for the number of potentially exchanged electrons, *i.e.* the amount of Ni^{+III} in the samples. Note that the stoichiometric NiO green sample exhibits very high $\Delta E/\Delta A$ slope, in agreement with our model. Surprisingly, the calculated γ_{tot} values are very dispersed as they go from 0.34–0.36 up to 2.38 J/m². The lower values are well falling within the range reported for oxides in contact with aqueous solutions,[22] but the higher ones are totally out of scale. It turned out that these unexpected overvalues correspond to all of the mosaic samples, thus having internal solid-solid interfaces
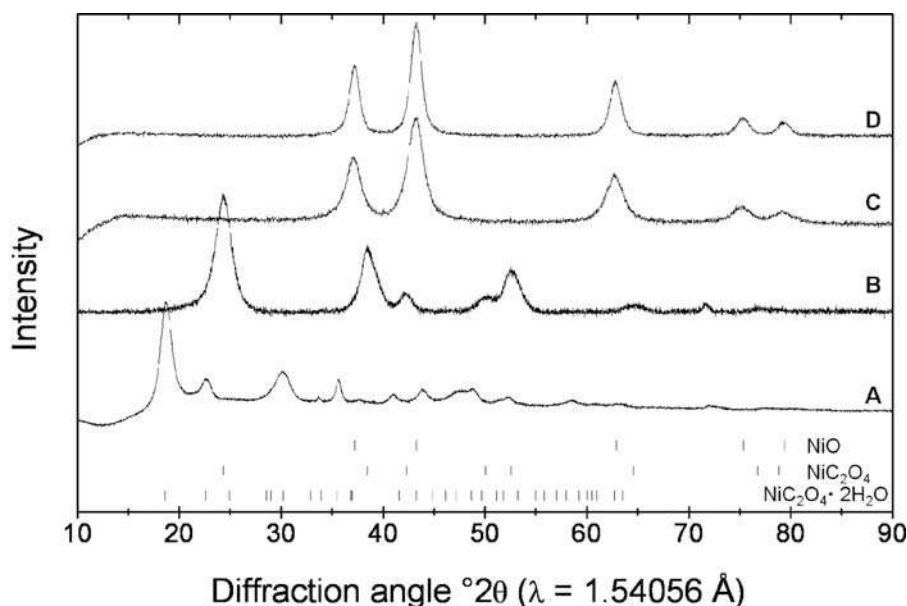
Figure 2. Evolution in XRD patterns upon air-heating of the $NiC_2O_4 \cdot 2H_2O$ precursor (A). Selected samples are NiO $_{20\,min}$ (B), NiO $_{40\,min}$ (C) and NiO $_{34\,h}$ (D).
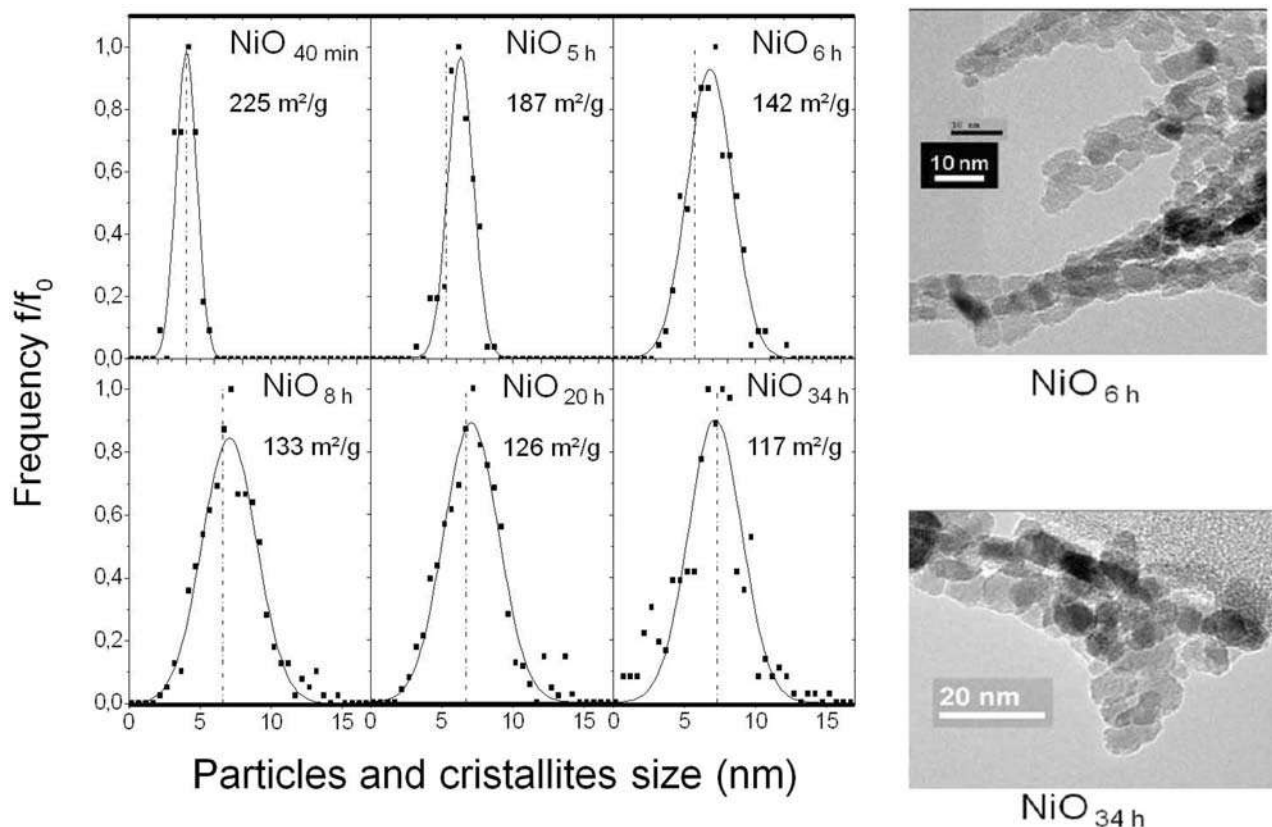
Figure 3. Particles size distribution (dots and curves) for selected NiO samples together with their crystallite size as deduced from XRD data (vertical dashed lines).

which related energy (γ_{SS}) likely contributes to the total interfacial energy in addition to the Solid-Liquid part (γ_{LS}). Note that higher the L_p-L_c difference, higher the measured γ_{tot} value, further emphasizing this inter-crystallite contribution. Also, solid-solid interfaces are reported to have much higher interfacial energies that solid-liquid ones,

in agreement with the trend herein observed. Direct confirmation of this point is presently checked by preparing micrometric powders comprising a high amount of solid-solid interfaces *i.e.* highly mosaic with low specific surface area. A larger panel of samples with varied textures is also presently prepared for a better statistic and more
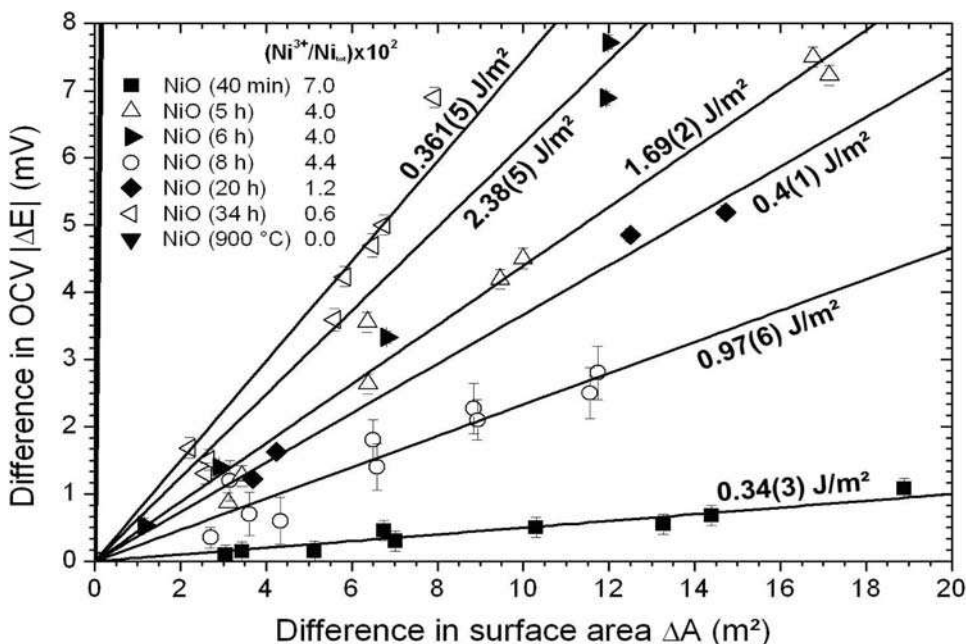
Figure 4. Evolution in the OCV (ΔE) values as a function of the difference in surface area (ΔA) between the two electrodes for different NiO samples. Numerical values are the specific total free energy (γ_{tot}) values deduced from the slope and Ni^{+III}/Ni$_{total}$.
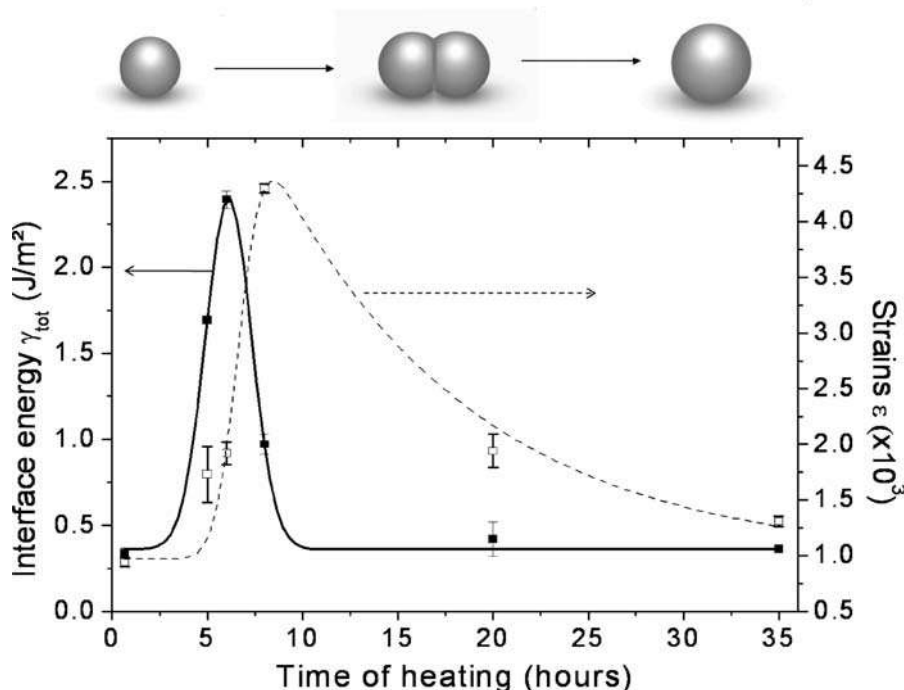
Figure 5. Evolution in the structural strains (ε) and total specific surface free energy (γ_tot) as a function of the heating time. Drawings schematize the size and textural particles evolution.

accurate access to energy contributions for mosaic samples. Indeed, we cannot in this case rule out a contribution of the structural stress (ε) to the γ value as both evolve very similarly (Figure 5).

Conclusions

Using an innovative but simple potentiometric experimental strategy, the surface free energy of NiO nano-particles in contact with an aqueous electrolyte has been determined (0.34–0.36 J/m^2). However, monolithic powders must be used in order to avoid additional contributions of inter-crystallites and structural stress. We are presently testing this methodology with other electrode materials and other organic solvents where only γ_LS will be affected. Worth noting is that surface/interface energies is not, until now, considered as a driving parameter for safety issues in the field of energy storage, but the use of downsizing materials will make this aspect certainly critical, hence the need of reliable *in situ* method. There is no doubt that samples with minimized interface free energy (*i.e.* rational choice of the solid/electrolyte couple) and low internal interfacial energy will have much improved long-term stability in electrochemical storage systems.

References

1. S. M. Myers and A. F. Wright, *J. of Appl. Phys.*, **90**, 5612 (2001).
2. P. M. Olivier, G. W. Watson, E. T. Kelsey, and S. C. Parker, *J. Mater. Chem.*, **7**, 563 (1997).
3. H. L. Skriver and N. M. Rosengaard, *Phys. Rev. B.*, **46**, 7157 (1992).
4. V. S. Markin, M. I. Gugeshashvili, A. G. Volkov, G. Munger, and R. M. Leblanc, *J. Colloid Interf. Sci.*, **154**, 264 (1992).
5. D. Chvedov and E. L. B. Logan, *Colloid Surface A*, **240**, 211 (2004).
6. B. B. Sauer and N. V. Dipaolo, *J. Colloid Interf. Sci.*, **144**, 527 (1991).
7. L. C. Chem and F. Spaepen, *J. Appl. Phys.*, **69**, 679 (1991).
8. A. Schroeder, J. Fleig, H. Drings, R. Wuerschum, J. Maier J, and W. Sitter, *Solid State Ionics*, **173**, 95 (2004).
9. P. Knauth, G. Schwitzgebel, A. Tscho, and S. Villain, *J. Solid State Chem.*, **140**, 295 (1998).
10. P. Balaya and J. Maier, *Phys. Chem. Chem. Phys.*, **12**, 215 (2010).
11. H. Sang and W. A. Miller, *J. Cryst. Growth.*, **6**, 303 (1970).
12. M. A. Meyers, A. Mishra, and D. J. Benson, *Prog. Mater. Sci.*, **51**, 427 (2006).
13. C. P. Gräf, U. Heim, and G. Schwitzgebel, *Solid State Ionics*, **131**, 165 (2000).
14. A. V. Virkar and Y. Zhou, *J. Electrochem. Soc.*, **154**, B540 (2007).
15. P. Knauth, *J. Solid State Electrochem.*, **5**, 107 (2001).
16. S. Andrieu and P. Müller, Les surfaces solides: concepts et méthodes, EDP Sciences, Les Ulis, 2005.
17. G. J. Li, X. X. Huang, Y. Shi, and J. K. Guo, *Mater. Lett.*, **51**, 325 (2001).
18. J. Laugier and A. Filhol, ERACEL program, CELREF (1978).
19. G. K. Williamson and W. H. Hall, *Acta Metall. Mater.*, **1**, 22 (1953).
20. S. Brunauer, P. H. Emmett, and E. Teller, *J. Am. Chem. Soc.*, **60**, 309 (1938).
21. F. Fievet, P. Germi, F. de Bergevin, and M. Figlarz, *J. Appl. Cryst.*, **12**, 387 (1979).
22. T. Hamieh, *C. R. Acad. Sci. II B.*, **325**, 353 (1997).